Numerical Method to Compute TE and TM Multiple Scatter from Rough Surfaces Exhibiting Backscatter Enhancement

Magda El-Shenawee, member IEEE, and Ezekiel Bahar, fellow IEEE
Electrical Engineering Department/Center for Electro-Optics
University of Nebraska, Lincoln, NE 68588-0511.

ABSTRACT - A Numerical method is presented to evaluate the full wave solutions for TE (horizontally polarized) and TM (vertically polarized) double scatter cross sections of one dimensional random rough surfaces. The full wave double scatter cross sections are expressed in terms of six dimensional integrals. The cpu time needed to evaluate the six dimensional integrals using standard techniques is excessive even for supercomputers. A numerical technique is used to reduce the six dimensional integrals into three dimensional integrals (one dimensional integral calling two independent two dimensional integrals). These two dimensional integrals account for the correlations between the heights and slopes at two points on the surface. The results exhibit the observed sharp enhanced backscatter and the polarization dependence of the cross sections. The angular width and the magnitude of the enhanced backscatter depend on the rough surface parameters (mean square height and slope).

I. Formulation Of The Problem

The random rough surfaces are assumed to be rough in one dimension y=h(x) and the medium y<h(x) is assumed to be a good conductor. The incident electromagnetic excitation is assumed to be TE or TM plane waves and the receiver is assumed to be located in the far field. For suppressed exp(jωt) time excitations, the full wave solutions for the diffuse double scattered far fields are given by [1],[2]

$$G_d^{fp}(\bar{r}) = \frac{k_0^4}{4\pi^2}\sqrt{\frac{2\pi}{k_0 r}}\exp\{j\pi/4 - jk_0 r\}\int \frac{D_{1'}(\bar{n}',\bar{n}^i)}{[k_0(-n_y^i+n_y')]}$$

$$\cdot\frac{D_{2'}(\bar{n}^f,\bar{n}')}{[k_0(n_y^f - n_y')]}\,U(\bar{r}_{s1}')\,U(\bar{r}_{s2}')\,\exp\{-jk_0 x_{s1}'(n_x^i - n_x')\}$$

$$\cdot[\exp\{-jk_0 h_1'(n_y^i - n_y')\} - 1]\exp\{jk_0 x_{s2}'(n_x^f - n_x')\}$$

$$\cdot[\exp\{jk_0 h_2'(n_y^f - n_y')\} - 1]\frac{dn_y'}{\sqrt{1-n_y'^2}}\,dx_{s1}'\,dx_{s2}', \quad (1)$$

in which the incident and the scatter wave vectors are in the directions of the unit vectors

$$\bar{n}^i = n_x^i\bar{a}_x + n_y^i\bar{a}_y, \text{ and } \quad \bar{n}^f = n_x^f\bar{a}_x + n_y^f\bar{a}_y, \quad (2)$$

Manuscript received November 1, 1993. This work was supported by the ARO under Grant No. DAAL03-87-0085.

The position vectors to point 1' and point 2' on the rough surface are given by $\bar{r}_{s1}'$ and $\bar{r}_{s2}'$, respectively, (see Fig.1)

$$\bar{r}_{s1}' = x_{s1}'\,\bar{a}_x + h_1'\,\bar{a}_y, \quad \bar{r}_{s2}' = x_{s2}'\,\bar{a}_x + h_2'\,\bar{a}_y, \quad (3)$$

The wave vector in the direction of the fields scattered from point 1' on the surface to point 2' on the surface is

$$\bar{k}_0' = k_0\bar{n}' = k_0(n_x'\bar{a}_x + n_y'\bar{a}_y), \quad (4)$$

in which the free space wave number is $k_0 = \omega\sqrt{\mu_0\epsilon_0}$ and $\bar{n}'$ is a unit vector. The surface element scattering coefficients at points $\bar{r}_{s1}'$ and $\bar{r}_{s2}'$ on the surface are $D_{1'}(\bar{n}',\bar{n}^i)$ and $D_{2'}(\bar{n}^f,\bar{n}')$, respectively. The scattering coefficients depend on the polarizations of the incident and scattered waves, the media on both sides of the rough surface, and the local normals $\bar{n}_1'$ and $\bar{n}_2'$ at these points on the surface [1] (see Fig. 1). The shadow function $U(\bar{r}_{s1}')$ is equal to one only if point 1' on the surface is illuminated by the incident plane wave and observed at point 2' on the surface. The shadow function $U(r_{s2}')$ is equal to one only if point 2' is illuminated by a point source at point 1' on the surface and visible by the receiver [3].

The double scattered intensity is obtained by multiplying the expression for the field (1) by its complex conjugate. The position vectors $\bar{r}_{s1}''$ and $\bar{r}_{s2}''$ associated with the complex conjugate fields are given by

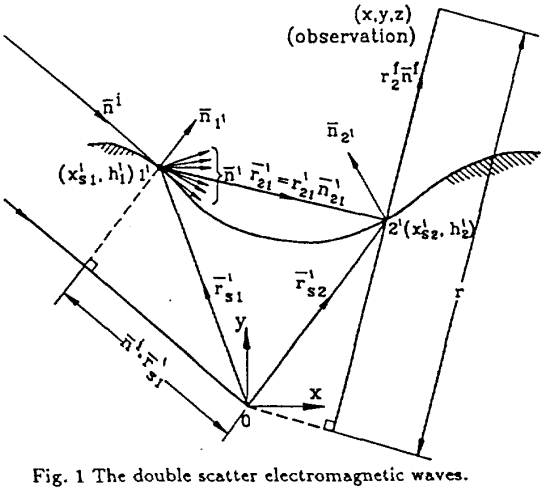

Fig. 1 The double scatter electromagnetic waves.

0018-9464/94$4.00 © 1994 IEEE

$$\bar{r}''_{s1} = x''_{s1}\,\bar{a}_x + h''_1\,\bar{a}_y, \qquad \bar{r}''_{s2} = x''_{s2}\,\bar{a}_x + h''_2\,\bar{a}_y, \quad (5)$$

and the wave vector in the direction of the conjugate scattered fields is

$$\bar{k}''_0 = k_0\bar{n}'' = k_0(n''_x\bar{a}_x + n''_y\bar{a}_y), \quad (6)$$

The major contributions to the double scattered intensity come from the quasi parallel and the quasi anti parallel paths for the field and its complex conjugate (see Fig. 2 a,b) [4]. The statistical averages of the intensities with respect to the random heights and slopes at two pairs of points on the surface involve the conditional joint characteristic functions [5]. For the quasi anti parallel case, the diffuse double scatter cross section is given by

$$\langle\sigma_d\rangle = \frac{k_0^7}{4\pi^2\,2L}\int < \Big[\frac{D_{1'}(\bar{n}',\bar{n}^i)\;D^*_{2''}(\bar{n}^f,\bar{n}'')}{[k_0(-n^i_y+n'_y)]\;[k_0(n^f_y-n''_y)]}$$

$$\cdot[\exp\{-jk_0h'_1(n^i_y-n'_y)\}-1]\;[\exp\{-jk_0h''_2(n^f_y-n''_y)\}-1]\Big]$$

$$\cdot\Big[\frac{D_{2'}(\bar{n}^f,\bar{n}')\;D^*_{1''}(\bar{n}'',\bar{n}^i)}{[k_0(n^f_y-n'_y)]\;[k_0(-n^i_y+n''_y)]}\;[\exp\{jk_0h'_2(n^f_y-n'_y)\}-1]$$

$$\cdot[\exp\{jk_0h''_1(n^i_y-n''_y)\}-1]\Big]\;U(\bar{r}'_{s1})\;U(\bar{r}'_{s2})\;U(\bar{r}''_{s1})\;U(\bar{r}''_{s2})>$$

$$\cdot\exp\{jk_0\tfrac{x_{d1}}{2}(n^f_x-n^i_x+n'_x-n''_x)\}\exp\{jk_0\tfrac{x_{d2}}{2}(n^f_x-n^i_x-n'_x+n''_x)\}$$

$$\cdot\exp\{jk_0x_m(n^f_x+n^i_x-n'_x-n''_x)\}\;\frac{dn'_y\,dn''_y}{\sqrt{1-n'^2_y}\sqrt{1-n''^2_y}}$$

$$\cdot dx_{d1}\,dx_{d2}\,dx_{c1}\,dx_{c2}\,, \quad (7)$$

where x_{di} and x_{ci} are $x_{di}=x'_{si}-x''_{sj}$ and $x_{ci}=(x'_{si}+x''_{sj})/2$ $(i\neq j=1,2)$. The random variables in (7) are the heights and the slopes at $\bar{r}'_{s1}$, $\bar{r}''_{s1}$, $\bar{r}'_{s2}$, and $\bar{r}''_{s2}$ on the surface and the shadow functions $U(\bar{r}'_{s1})$, $U(\bar{r}'_{s2})$, $U(\bar{r}''_{s1})$, and $U(\bar{r}''_{s2})$. The rough surface is assumed to be characterized by a Gaussian joint probability density function for the surface heights and slopes at two pairs of points on the surface. The surface height autocorrelation function and its Fourier transform (the rough surface spectral density function) are also assumed to be Gaussian. The standard large radii of curvature assumption is made and the height slope correlations are accounted for through the use of the conditional joint characteristic functions [5]. The rough surface variables x_{c1} and x_{c2} are expressed in terms of $x_c=(x_{c1}+x_{c2})/2$ and $x_m=x_{c1}-x_{c2}$. The limits of x_c and x_m are $(-L,L)$ and $(-L_m,L_m)$, respectively. The distance L_m is the statistical average of mean path for the double scattered waves. The quasi parallel and the quasi anti-parallel contributions to the diffuse double scatter cross sections are expressed in terms of six dimensional integrals [6]. The quasi anti-parallel contribution to the diffuse double scatter cross section is

$$\langle\sigma_{ad}\rangle = \frac{k_0^7}{4\pi^2}(2L_m)\;P_2(\bar{n}^i)\;P_2(\bar{n}^f)\int\int\langle\sigma_{ad_1}(n'_y,n''_y)\rangle$$

$$\cdot\langle\sigma_{ad_2}(n'_y,n''_y)\rangle\;\mathrm{sinc}\{k_0L_m(n^f_x+n^i_x-n'_x-n''_x)\}$$

$$\cdot\exp\{-k_0^2\langle h^2\rangle(-n^i_y+n'_y-n^f_y+n''_y)^2\}$$

$$\cdot[1-P_2(|n'_y|)]\;[1-P_2(|n''_y|)]\;\frac{dn'_y\,dn''_y}{\sqrt{1-n'^2_y}\sqrt{1-n''^2_y}}, \quad (8a)$$

in which $\langle\sigma_{ad_1}(n'_y,n''_y)\rangle$ and $\langle\sigma_{ad_2}(n'_y,n''_y)\rangle$ are associated with the single scatter cross sections.

$$\langle\sigma_{ad_1}(n'_y,n''_y)\rangle = 2\int\int\Big[\frac{\mathrm{Re}\{D_{1'}(\bar{n}',\bar{n}^i)\;D^*_{2''}(\bar{n}^f,\bar{n}'')\}}{[k_0(-n^i_y+n'_y)]\;[k_0(n^f_y-n''_y)]}$$

$$\cdot\cos\{k_0[\tfrac{x_{d1}}{2}(n^f_x-n^i_x+n'_x-n''_x)+h_{xc1}\frac{B_1}{\langle h^2_x\rangle}(n^f_y-n^i_y+n'_y-n''_y)]\}$$

$$\cdot\exp\{-k_0^2(-n^i_y+n'_y)(n^f_y-n''_y)[\langle h^2\rangle(1-R_1)-\frac{2B_1^2}{\langle h^2_x\rangle}]\}$$

$$\cdot\exp\{\frac{k_0^2\,B_1^2}{2\langle h^2_x\rangle}(-n^i_y+n'_y-n^f_y+n''_y)^2\}$$

$$\cdot p(h_{xc1})\,dh_{xc1}\,dx_{d1}, \quad (8b)$$

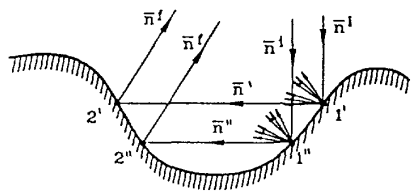

Fig.2-a Quasi-parallel, regular path $\bar{n}'\approx\bar{n}''$

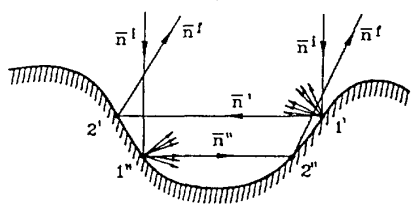

Fig.2-b Quasi-antiparallel, cross path $\bar{n}'\approx-\bar{n}''$

and

$$<\sigma_{ad2}(n'_y,n''_y)>=2\int\int\left[\frac{\mathrm{Re}\left\{D^*_{1''}(\bar{n}'',\bar{n}^i)\,D_{2'}(\bar{n}^f,\bar{n}')\right\}}{[k_0(-n^i_y+n''_y)]\,[k_0(n^f_y-n'_y)]}\right.$$

$$\cdot\cos\{k_0[\frac{x_{d2}}{2}(n^f_x-n^i_x-n'_x+n''_x)+h_{xc2}\frac{B_2}{<h^2_x>}(n^f_y-n^i_y-n'_y+n''_y)]\}$$

$$\cdot\exp\{-k_0^2(-n^i_y+n''_y)(n^f_y-n'_y)[<h^2>(1-R_2)-\frac{2B_2^2}{<h^2_x>}]\}$$

$$\cdot\exp\{\frac{k_0^2\,B_2^2}{2<h^2_x>}(-n^i_y+n''_y-n^f_y+n'_y)^2\}$$

$$\left.\cdot p(h_{xc2})\,dh_{xc2}\,dx_{d2},\right. \qquad (8c)$$

A similar expression is obtained for the contribution from the quasi parallel path. At high frequencies, $[1-P_2(|n'_y|)]$ and $[1-P_2(|n''_y|)]$ are the probabilities of a multiple scatter event, where P_2 is derived by Sancer [3]. Similarly, the probabilities that the surface will be illuminated by the incident wave and visible in the scatter direction are given by $P_2(\bar{n}^i)$ and $P_2(\bar{n}^f)$, respectively [3]. In (8b) and (8c), the probability density functions for the slopes h_{xc1} and h_{xc2} at the mid points between 1′ and 2″, and between 2′ and 1″ are $p(h_{xc1})$ and $p(h_{xc2})$, respectively. The limits of integration for x_{d1} and x_{d2} are (0,2L). The correlations between the heights and the slopes at the points 1′ and 2″ and at the points 2′ and 1″ on the surface are given by B_1 and B_2, respectively, and R_1 and R_2 are the surface height autocorrelation functions at these pairs of points. The mean square height and slope of the surface are given by $<h^2>$ and $<h^2_x>$, respectively. The corresponding expression for the coherent intensity $<\sigma_c>$ is obtained from (8) on setting $R_{1,2}$ and $B_{1,2}$ equal to zero. The incoherent diffuse scatter cross section is $<\sigma_I>=<\sigma_d>-<\sigma_c>$.

For the propagating waves, the range of integration for n'_y and n''_y are (-1,1). Notice that the integrand in (8) is equal to its complex conjugate when $\bar{n}'$ and $\bar{n}''$ are interchanged. Thus instead of integrating with respect to n'_y and n''_y over (-1,1), it is sufficient to integrate twice the real part of the integrand over the region $n'_y \geq n''_y$. To evaluate (8) new variables of integrations n_{ay} and n_{dy} are introduced in (8a) instead of n'_y and n''_y. They are given by

$$\bar{n}_a=\frac{\bar{n}'+\bar{n}''}{2},\ \text{and}\qquad \bar{n}_d=\bar{n}'-\bar{n}'' \qquad (9)$$

The region of integration over n_{ay} and n_{dy} is a diamond shaped area whose end points on the n_{dy} axis are ± 2 and on the n_{ay} axis are ± 1. The integration is performed over the region $n_{dy} \geq 0$ (corresponding to the region $n'_y \geq n''_y$). In (8b) and (8c) it is necessary to account for $n'_x>0$, $n''_x<0$ as well as for $n'_x<0$, $n''_x>0$ for the quasi anti-parallel case. The integrands of the quasi parallel and the quasi anti parallel double scatter cross sections are plotted as functions of the wave vector variables [6]. These results show that the major contributions to the double scatter integrals come from the region around $\bar{n}'=\bar{n}''$ for the quasi parallel case and from the region around $\bar{n}'=-\bar{n}''$ for the quasi anti parallel case. Moreover in view of the factors $(1-P_2)$ (associated with the multiple scatter events), the integrand of (8a) peaks when $n'_y=0$ and $n''_y=0$. Thus for the quasi anti parallel paths, the integrals (8b) and (8c) are evaluated numerically as functions of n_{dy} for $n'_y=-n''_y=n_{dy}/2$ ($n_{ay}=0$). The integrand of (8a) is evaluated as a function of n_{dy} and n_{ay} without recomputing (8b) and (8c). Thus the six dimensional integrals for the quasi parallel and the quasi anti parallel cross sections are for practical purpose reduced to three dimensional integrals using this numerical technique.

II. Illustrative Examples

The diffuse single and double (quasi parallel+quasi anti-parallel) scatter incoherent cross sections are plotted as functions of the scatter angles ($\theta^f\cos\phi^f$ for $\phi^i=0,\phi^f=0,\pi$) for the vertically (TM) and horizontally (TE) polarized waves. The total cross section in obtained by adding the single and the double cross sections incoherently. The probability density functions of the slopes are assumed to be Gaussian. The mean square slope is $<h^2_x>=0.508$ and the surface correlation length is $l_c=3.34$ μm. In Fig. 3 the free space wave length is $\lambda=1.152$ μm and in Figs. 4 and 5 the wave length is $\lambda=3.392$ μm. The relative complex permittivity of the medium $y<h(x)$ is $\epsilon_r=-62.787-j4.948$ at $\lambda=1.152$ μm. It is $\epsilon_r=-424.64-j81.144$ at $\lambda=3.392$ μm. The double scatter mean path is $L_m=11.13l_c$ [6]. The incident angle is $\theta^i=10°$. The results show sharp enhancement in the backscatter direction due to contributions from the quasi anti parallel double scatter paths. The polarization dependence is shown in Fig. 5. It is primarily due to the differences in the double scatter cross sections. Notice that the angular width of the enhancement around the backscatter direction is larger in Fig.4 than in Fig. 3. However, the level of the enhancement is larger in Fig. 3.

III. Conclusions

The six dimensional integral expressions for the double scatter cross sections are evaluated as three dimensional integrals. The sharp enhanced backscatter is associated with the contributions from the quasi-anti parallel double scatter path. The double scatter cross sections depend upon the polarization. The angular

width and the magnitude of the sharp enhanced backscatter depend on the frequency and the rough surface parameters. These results are significantly different from the corresponding physical optics approximations.

ACKNOWLEDGMENT

The computational work was conducted at Cornell National Supercomputer Facility supported by NSF.

REFERENCES

[1] M. El-Shenawee, "Full wave multiple scattering and depolarization of electromagnetic fields from rough surfaces," Ph. D. dissertation in electrical engineering, University of Nebraska-Lincoln, August 1991.

[2] E. Bahar and M. El-Shenawee, "Use of supercomputers to evaluate singly and doubly scattered electromagnetic fields from rough surfaces," IEEE Trans. on Magnetics, vol. 27, no. 5, pp. 4287-4290, September 1991.

[3] M. I. Sancer, "Shadow-correlated electromagnetics scattering from a randomly rough surface," IEEE Trans. Ant. and Propagat., vol. Ap-17, no. 5, pp. 577-585, September 1969.

[4] A. Ishimaru and Jei S. Chen, "Scattering from very rough surfaces based on the modified second order Kirchoff approximation with angular and propagation shadowing," J. Acoust. Soc. Am. 88 (4), pp. 1877-1883, October 1990.

[5] E. Bahar, "Full wave analysis for rough surface diffuse incoherent radar cross sections with height slope correlations included," IEEE Trans. on Ant. and Propagat., vol. 39, no. 9, pp. 1293-1304, September 1991.

[6] E. Bahar and M. El-Shenawee, "Full wave multiple scattering from one dimensional random rough surfaces and high frequency stationary phase approximations," Proceedings of IEEE Antenna and Propagation Society International Symposium, pp. 1316-1319, July 1993.

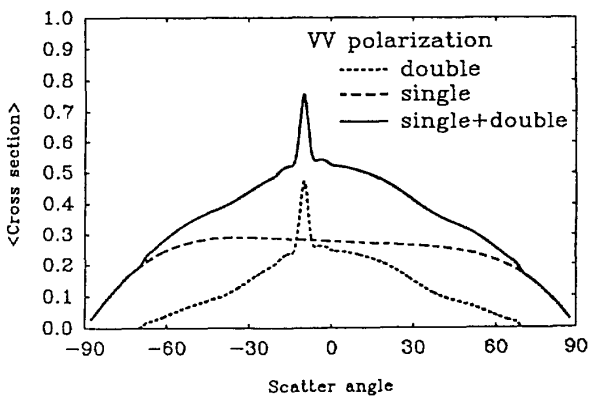

Fig. 3. Cross sections versus scatter angle ($\theta^l \cos\phi^l$), $\phi^l = 0, \pi$. For $\theta^i = 10°$, $\phi^i = 0$, $\langle h_x^2 \rangle = 0.508$, $\lambda = 1.152\mu m$, $\epsilon_r = -62.787 - j4.948$.

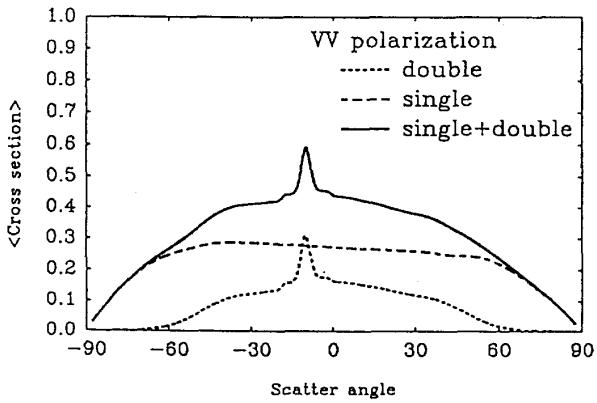

Fig. 4. Cross sections versus scatter angle ($\theta^l \cos\phi^l$), $\phi^l = 0, \pi$. For $\theta^i = 10°$, $\phi^i = 0$, $\langle h_x^2 \rangle = 0.508$, $\lambda = 3.392\mu m$, $\epsilon_r = -424.648 - j81.144$.

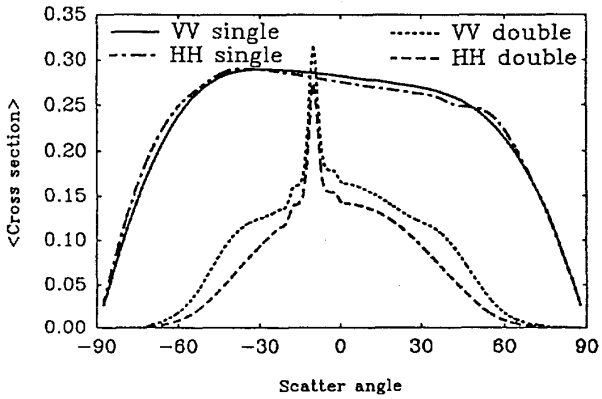

Fig. 5. Cross sections versus scatter angle ($\theta^l \cos\phi^l$), $\phi^l = 0, \pi$. For $\theta^i = 10°$, $\phi^i = 0$, $\langle h_x^2 \rangle = 0.508$, $\lambda = 3.392\mu m$, $\epsilon_r = -424.648 - j81.144$.